Bounding the distance between 2D parametric Bézier curves and their control polygon

M.I. Karavelas* P.D. Kaklis† K.V. Kostas†

Abstract

Employing the techniques presented by Nairn, Peters and Lutterkort in [1], sharp bounds are firstly derived for the distance between a planar parametric Bézier curve and a parameterization of its control polygon based on the Greville abscissae. Several of the norms appearing in these bounds are orientation dependent. We next present algorithms for finding the optimal orientation angle for which two of these norms become minimal. The use of these bounds and algorithms for constructing polygonal envelopes of planar polynomial curves, is illustrated for an open and a closed composite Bézier curve.

1 Introduction

The aim of this paper is to exploit the results presented in Nairn, Peters and Lutterkort [1], for deriving bounds between a two-dimensional *parametric* Bézier curve of degree d and its control polygon. In [1] the authors achieve in deriving sharp and easily computable bounds on the maximum distance between a *functional* Bézier segment and its control polygon. Using a different approach, Reif [2] derived, at the same time and independently of [1], a bounding function that is sharp everywhere.

The bounds in [1] are expressed in terms of the first- or second-order differences of the control-point sequence and a constant depending only on

*University of Notre Dame, Dept. Computer Science and Engineering, Notre Dame, IN 46556, U.S.A.; email: `mkaravel@cse.nd.edu`

†National Technical University of Athens, Dept. Naval Arch. & Mar. Eng., Greece; emails: {`kaklis,kostas`}`@deslab.ntua.gr`

the degree of the polynomial. These bounds permit confining a Bézier segment within a polygonal region, consisting of at most $2d+2$ line segments, which is considerably finer in comparison to the convex-hull estimate. As a consequence, they can improve the efficiency of several CAGD algorithms for, e.g., detecting collision between 2D bodies, creating tolerance envelopes, etc. Their applicability range is, however, restricted from the fact that they deal with functional curves and thus, if applied in the parametric case, the resulting envelopes will be in general orientation dependent.

In the present paper we first develop a straightforward generalization of the method in [1] for planar parametric Bézier segments $\mathbf{r}(t)$, $t\in[0,1]$. For this purpose we measure the distance between $\mathbf{r}(t)$ and its control polygon $\mathbb{L}$ by $\max_{t\in[0,1]} \|\mathbf{r}(t) - \ell(t)\|_p$, $p\geq 1$, where $\ell(t)$ is a piecewise linear parameterization of $\mathbb{L}$ with knot vector induced by the Greville abscissae. In §2 we derive bounds of the afore-mentioned distance, expressed in terms of the p-norm of the second-order differences of the control-point sequence and constants depending only on the degree d, which are shown to be sharp for all degrees. The section ends with deriving, again by adopting the approach in [1], improvements of the bounds near the endpoints of an open curve.

Several of the norms appearing in the bounds of §2 are orientation dependent. In §3 we rationally select two of these norms and develop algorithms for determining the optimal orientation angle for which they become minimal. The total running time of these algorithms is estimated to be of $O(d^2\alpha(d))$, where $\alpha(d)$ denotes the functional inverse of Ackermann's function. Note that $\alpha(d)$ is a very slowly growing function of d, and its value is 4 for all reasonable[1] values of d.

The paper concludes in §4, which illustrates the use of the results and techniques presented in §2 and §3, for constructing tight polygonal envelopes of planar polynomial curves. These envelopes are expressed as the Minkowski sum of the parameterization $\ell(t)$ of the control polygon of the curve and a closed set, whose shape and extent are determined from the bound we use.

2 Alternative bounds

As it is well known, a two-dimensional parametric Bézier curve of degree d is representable as $\mathbf{r}(t) = \sum_{i=0}^{d} \mathbf{b}_i B_i^d(t), \quad t \in [0,1]$, where $B_i^d(t)$ is the i-th

[1]Note that $\alpha(n) \geq 4$ for all $n \leq M$, where M is a exponential tower with 65536 2's; thus $\alpha(n) \leq 4$ for all practical values of n.

Bernstein polynomial of degree d and $\mathbf{b}_i$, $i = 0, \ldots, d$, are the so-called *control points* of $\mathbf{r}(t)$. The *control polygon* $\mathbb{L}$ of $\mathbf{r}(t)$ is the polygonal line connecting the control points $\mathbf{b}_i$ according to the order implied by the subscript i. We parameterize the polygon $\mathbb{L}$ with the aid of the Greville abscissae $t_k = \frac{k}{d}$ as follows: the restriction of the parameterization $\ell(t)$ of $\mathbb{L}$ on the segment $[t_k, t_{k+1}]$ is defined as:

$$\ell_{[t_k,t_{k+1}]}(t) = \mathbf{b}_k \frac{t_{k+1} - t}{t_{k+1} - t_k} + \mathbf{b}_{k+1} \frac{t - t_k}{t_{k+1} - t_k}, \tag{1}$$

where $t \in [t_k, t_{k+1}]$ and $k = 0, 1, \ldots, d-1$. The purpose of this section is to derive good, if possible sharp, upper bounds on the distance between the Bézier curve $\mathbf{r}(t)$, $t \in [0,1]$, and the parameterization $\ell(t)$ of the control polygon, the distance being measured by

$$\|\mathbf{r}(t) - \ell(t)\|_{\infty,p,[0,1]} = \max_{t\in[0,1]} \|\mathbf{r}(t) - \ell(t)\|_p = \max_{0\le k\le d-1} \max_{t\in[t_k,t_{k+1}]} \|\mathbf{r}(t) - \ell(t)\|_p, \tag{2}$$

where $\| \cdot \|_p$ denotes the p-norm in $\mathbb{R}^2$, $p \geq 1$. This purpose can be achieved by employing the methodology in [1] for functional Bézier curves. To start with, the difference $\mathbf{r}(t) - \ell(t)$ in the k-th subinterval $[t_k, t_{k+1}]$ is written in the form:

$$\mathbf{r}(t) - \ell(t) = \sum_{i=0}^{d} \mathbf{b}_i \alpha_{ki}(t), \quad t \in [t_k, t_{k+1}], \tag{3}$$

where

$$\alpha_{ki}(t) = B_i^d(t) - \begin{cases} k+1-dt & \text{if } i = k, \\ dt - k & \text{if } i = k+1, \\ 0 & \text{else.} \end{cases} \tag{4}$$

Appealing to the proof of [1, Theorem 3.1], the functions $\alpha_{ki}(t)$, $1 \leq i \leq d-1$, can be expressed as the second-order centered differences of the non-negative quantities

$$\beta_{ki}(t) := \sum_{j=0}^{i} (i-j)\alpha_{kj}(t) = \begin{cases} \sum_{j=0}^{i} (i-j) B_j^d(t) & \text{for } 0 \leq i \leq k, \\ \sum_{j=i}^{d} (j-i) B_j^d(t) & \text{for } d \geq i \geq k+1, \end{cases} \tag{5}$$

that is

$$\alpha_{ki}(t) = \Delta_2 \beta_{ki}(t) = \beta_{k,i+1}(t) - 2\beta_{ki}(t) + \beta_{k,i-1}(t), \quad 1 \leq i \leq d-1. \tag{6}$$

The validity of (6) can be extended to include $i = 0, d$. Firstly, it is readily noted from (5) that $\beta_{k0}(t) = 0$ and $\alpha_{k0}(t) = \beta_{k1}(t)$. Secondly, on the basis that $\sum_{j=0}^{d} \alpha_{kj}(t) = 0$, which stems easily from (4), we can prove $\alpha_{kd}(t) = \beta_{k,d-1}(t)$. Thirdly, again from (5), we can readily show that $\beta_{kd}(t) = 0$. Then, if we set $\beta_{k,-1}(t) = \beta_{k,d+1}(t) := 0$, the validity range of (6) can be extended as $\alpha_{ki}(t) = \Delta_2\beta_{ki}(t), \quad 0 \leq i \leq d$. Substituting now into the right-hand side of (3), and transferring the difference operator Δ_2 from $\beta_{ki}(t)$ to $\mathbf{b}_i$, we arrive at the following expression

$$\mathbf{r}(t) - \ell(t) = \sum_{i=1}^{d-1} \beta_{ki}(t)\Delta_2\mathbf{b}_i, \quad t \in [t_k, t_{k+1}]. \tag{7}$$

Combining now (7) with (2) and using the triangle inequality, we get

$$\|\mathbf{r}(t) - \ell(t)\|_{\infty,p,[0,1]} \leq \max_{0\leq k\leq d-1} \max_{t\in[t_k,t_{k+1}]} \sum_{i=1}^{d-1} \beta_{ki}(t)\|\Delta_2\mathbf{b}_i\|_p, \tag{8}$$

where the fact that $\beta_{ki}(t)$ are non-negative, has also been taken into account. Then, using Hölder's inequality for further bounding the sum in the right-hand side of (8), we obtain:

Theorem 2.1 *The distance* $\|\mathbf{r}(t) - \ell(t)\|_{\infty,p,[0,1]}$ *is bounded above as*

$$\|\mathbf{r}(t) - \ell(t)\|_{\infty,p,[0,1]} \leq \mathtt{N}_r(d)\|\Delta_2\mathbf{b}\|_{rp}, \qquad p\geq 1, r = 1, \infty, \tag{9}$$

where

$$\mathtt{N}_1(d) = \max_{0\leq k\leq d-1} \max_{t\in[t_k,t_{k+1}]} \max_{1\leq i\leq d-1} \beta_{ki}(t), \quad \|\Delta_2\mathbf{b}\|_{1p} = \sum_{i=1}^{d-1} \|\Delta_2\mathbf{b}_i\|_p, \tag{10}$$

or

$$\mathtt{N}_\infty(d) = \max_{0\leq k\leq d-1} \max_{t\in[t_k,t_{k+1}]} \sum_{i=1}^{d-1} \beta_{ki}(t), \quad \|\Delta_2\mathbf{b}\|_{\infty p} = \max_{1\leq i\leq d-1} \|\Delta_2\mathbf{b}_i\|_p. \tag{11}$$

Next, we turn to investigate the sharpness properties of the above bounds. If we restrict ourselves to quadratic curves ($d = 2$), inequality (8) becomes strict equality: $\|\mathbf{r}(t) - \ell(t)\|_{\infty,p,[0,1]} = \|\Delta_2\mathbf{b}_1\|_p \max_{0\leq k\leq 1} \max_{t\in[t_k,t_{k+1}]} \beta_{k1}(t)$. On the other hand, setting $d = 2$ in (10) and (11) we get, for $r = 1, \infty$,

$\mathtt{N}_r(2) = \max_{0\le k\le 1}\max_{t\in[t_k,t_{k+1}]}\beta_{k1}(t)$, and $\|\Delta_2\mathbf{b}\|_{rp} = \|\Delta_2\mathbf{b}_1\|_p$, respectively. In view of the above equalities, we conclude that the bounds of Theorem 2.1 are sharp for degree $d = 2$.

We now consider the representation $\mathbf{r}^e(t)$ of quadratic Bézier curves after e degree elevations. It is then well known that all second-order difference vectors $\Delta_2\mathbf{b}_i^e$ are equal to each other, that is

$$\Delta_2\mathbf{b}_i^e = \Delta_2\mathbf{b}_1^e, \qquad i = 1,\dots,e+1,\ e\ge 1. \tag{12}$$

Then equality (7), in conjunction with (2), leads to

$$\|\mathbf{r}^e(t)-\ell(t)\|_{\infty,p,[0,1]} = \|\Delta_2\mathbf{b}_1^e\|_p \max_{0\le k\le e+1}\max_{t\in[t_k,t_{k+1}]}\sum_{i=1}^{e+1}\beta_{ki}(t). \tag{13}$$

Appealing to the bound (9; $r=\infty$), we note that the quantities in (11) take the following specific form

$$\mathtt{N}_\infty(2+e) = \max_{0\le k\le e-1}\max_{t\in[t_k,t_{k+1}]}\sum_{i=1}^{e+1}\beta_{ki}(t), \qquad \|\Delta_2\mathbf{b}^e\|_{\infty p} = \|\Delta_2\mathbf{b}_1^e\|_p. \tag{14}$$

Comparing (13) with the bound obtained after substituting the quantities in (14) into the right-hand side of (9; $r=\infty$), we deduce that the bound (9; $r=\infty$) of Theorem 2.1 is sharp for all degrees.

Aiming to extend the validity of the above result also for (9; $r=1$) as well, we first recall from [1, Theorem 4.1] that

$$\mathtt{N}_1(d) = \beta_{\lceil\frac{d}{2}\rceil\lceil\frac{d}{2}\rceil}(t^*), \quad t^* = \frac{\lceil\frac{d}{2}\rceil}{d}, \tag{15}$$

where $\lceil\cdot\rceil$ denotes the ceiling function. Then, if we restrict ourselves to the family of Bézier curves, denoted by $\hat{\mathbf{r}}(t)$, whose control polygon has the shape of an angle, more accurately

$$\Delta_2\hat{\mathbf{b}}_i = \mathbf{0} \quad \text{for} \quad i \ne \lceil\frac{d}{2}\rceil \quad \text{while} \quad \Delta_2\mathbf{b}_{\lceil\frac{d}{2}\rceil} \ne \mathbf{0}, \tag{16}$$

equality (7) degenerates to

$$\hat{\mathbf{p}}(t)-\ell(t) = \beta_{k\lceil\frac{d}{2}\rceil}(t)\Delta_2\hat{\mathbf{b}}_{\lceil\frac{d}{2}\rceil}. \tag{17}$$

Applying the $\|\cdot\|_{\infty,p,[0,1]}$ operator (see equ. (2)) on both sides of (17) and recalling (10) and (15), we arrive at

$$\|\hat{\mathbf{r}}(t) - \ell(t)\|_{\infty,p,[0,1]} = \mathtt{N}_1(d)\|\Delta_2 \hat{\mathbf{b}}_{\lceil \frac{d}{2} \rceil}\|. \tag{18}$$

It is then readily seen that, if (16) holds true, the right-hand side of both (9; $r = 1$) and (18) coincide. We can thus deduce that the bound (9; $r = 1$) of Theorem 2.1 is sharp for all degrees. Hence, we can state:

Theorem 2.2 *The bounds of Theorem 2.1 are sharp for all degrees.*

Recall that Theorem 2.1 is obtained by bounding the distance between a Bézier curve $\mathbf{r}(t)$, $t \in [0,1]$, and the parameterization $\ell(t)$ (see (1)) of its control polygon, measured via the norm $\|\cdot\|_{\infty,p,[0,1]}$, defined by (2). The bounding process involved employing successively the triangle and Hölder's inequality. An alternative approach could be to refrain from applying Hölder's inequality. Instead, one can stop at inequality (8), resulting from (7) with the aid of the triangle inequality, and note that the functions $\beta_{ki}(t)$, $i = 1,\ldots,d-1$, are not only non-negative but convex upwards as well; see [1, Fig.3]. It is then clear that this property is shared by the right-hand side of (8), enabling us to write

$$\max_{t\in[t_k,t_{k+1}]} \sum_{i=1}^{d-1} \beta_{ki}(t)\|\Delta_2 \mathbf{b}_i\|_p = \max_{j=k,k+1} \sum_{i=1}^{d-1} \beta_{ki}(t_j)\|\Delta_2 \mathbf{b}_i\|_p. \tag{19}$$

Appealing once again to [1, Fig.3], we introduce the functions

$$\beta_i(t) := \beta_{ki}(t), \quad t \in [t_k, t_{k+1}], \quad k = 0,1,\ldots,d-1,\ i = 1,\ldots,d-1, \tag{20}$$

for which it is straightforward to show that

$$\beta_i(t) \in C[0,1] \quad \text{with} \quad \beta_i(0) = \beta_i(1) = 0, \ \ i = 1,\ldots,d-1. \tag{21}$$

Then, by virtue of (20) and the first of (21), (19) can be written as

$$\max_{t\in[t_k,t_{k+1}]} \sum_{i=1}^{d-1} \beta_{ki}(t)\|\Delta_2 \mathbf{b}_i\|_p = \max_{j=k,k+1} \sum_{i=1}^{d-1} \beta_i(t_j)\|\Delta_2 \mathbf{b}_i\|_p. \tag{22}$$

Substituting (22) into the right-hand side of (8) and taking into account the second of (21), we obtain the following:

Theorem 2.3 *The distance* $\|\mathbf{r}(t) - \ell(t)\|_{\infty,p,[0,1]}$ *is bounded above as*

$$\|\mathbf{r}(t) - \ell(t)\|_{\infty,p,[0,1]} \le \max_{1\le k\le d-1} \sum_{i=1}^{d-1} \beta_i(t_k)\|\Delta_2 \mathbf{b}_i\|_p \tag{23}$$

with $\beta_i(t)$ *defined by (20) and (5).*

Coming to the sharpness issue for the previous bound, we select the family of Bézier curves, whose control polygons possess the property

$$\Delta_2 \mathbf{b}_i = \lambda_i \mathbf{c}, \quad \lambda_i \ge 0, \ \ i = 1, \dots, d-1, \tag{24}$$

for some constant vector $\mathbf{c} \ne \mathbf{0}$. If (24) holds true, then we need not resort to the triangle inequality for obtaining (8) from (7). Consequently, (8) holds true as equality for the curve family (24). The same can be said for (23), since no inequality strengthening is taking place during the elaboration from (22) to (23). Summarizing we can state

Theorem 2.4 *The bound of Theorem 2.3 is sharp for all degrees.*

It is worth-noticing that the curve family (24) contains those families for which the bounds of Theorem 2.1 have been shown to be sharp, namely the quadratic Bézier curves ($d = 2$), their degree-raised representation ($\lambda_i = \lambda, \ i = 1, \dots, d-1$) as well as the curves with angle-shaped polygon ($\lambda_i = 0$ for all $i \ne \lceil \frac{d}{2} \rceil, \ \lambda_{\lceil \frac{d}{2} \rceil} \ne 0$). Finally, it is straightforward to prove that every Bézier curve, fulfilling (24), is locally convex.

We end this section by providing a bound via those derived in [1] for functional Bézier curves. Setting $\mathbf{r}(t) = (r_x(t), r_y(t))^T$, $\ell(t) = (\ell_x(t), \ell_y(t))^T$, we can write

$$\|\mathbf{r}(t) - \ell(t)\|_{\infty,1,[0,1]} = \|p_x(t) - \ell_x(t)\|_{\infty,[0,1]} + \|p_y(t) - \ell_y(t)\|_{\infty,[0,1]}. \tag{25}$$

Then, appealing to [1, Theorem 3.1] and setting $\mathbf{b}_i = (b_{ix}, b_{iy})^T$, we get

Theorem 2.5 *The distance* $\|\mathbf{r}(t) - \ell(t)\|_{\infty,1,[0,1]}$ *is bounded above as*

$$\|\mathbf{r}(t) - \ell(t)\|_{\infty,1,[0,1]} \le N_\infty(d)(\|\Delta_2 b_x\|_\infty + \|\Delta_2 b_y\|_\infty) \tag{26}$$

where

$$\|\Delta_2 b_\bullet\|_\infty = \max_{1\le i\le d-1} \|\Delta_2 b_{i\bullet}\|_\infty, \quad \bullet = x, y. \tag{27}$$

The above bound degenerates to that in [1, Theorem 3.1] for functional curves, since in this case either of $\|\Delta_2 b_x\|_\infty$ or $\|\Delta_2 b_y\|_\infty$ is zero. Recalling now that the functional bound is sharp (see [1, Corollary 3.1]), we can state

Theorem 2.6 *The bound of Theorem 2.5 is sharp for all degrees.*

The bounds derived above can be improved near the endpoint $\mathbf{r}(0) = \mathbf{b}_0$ and, symmetrically, at $\mathbf{r}(1) = \mathbf{b}_d$. The first order Taylor expansion of $\mathbf{r}(t)$ at $t = 0$ is $\mathbf{r}(0) + \nabla\mathbf{r}(0)t$, which agrees with the first leg of the control polygon, parameterized by $(1 - dt)\mathbf{b}_0 + dt\mathbf{b}_1$. Hence, for $t \in [0, 1/d]$ and $\xi_x(t)$, $\xi_y(t) \in (0, t)$, we have

$$\begin{aligned}
\|\mathbf{r}(t) - \ell(t)\|_p &= \left[\left|\frac{p_x''(\xi_x(t))}{2}t^2\right|^p + \left|\frac{p_y''(\xi_y(t))}{2}t^2\right|^p\right]^{1/p} \\
&\le \frac{t^2}{2^{1-1/p}} \max\{|p_x''(\xi_x(t))|, |p_y''(\xi_y(t)|\} \\
&\le \frac{t^2}{2^{1-1/p}} d(d-1) \max\{\|\Delta_2 b_x\|_\infty, \|\Delta_2 b_y\|_\infty\} \\
&\le \frac{d(d-1)}{2^{1-1/p}} \|\Delta_2 \mathbf{b}\|_{\infty p} t^2 \\
&\le \frac{d-1}{2^{1-1/p}} \|\Delta_2 \mathbf{b}\|_{\infty p} t.
\end{aligned}$$

Working analogously for the bound (26) of Theorem 2.5, we get

$$\|\mathbf{r}(t) - \ell(t)\|_1 \le \frac{d-1}{2}(\|\Delta_2 b_x\|_\infty + \|\Delta_2 b_y\|_\infty)t, \qquad t \in [0, 1/d].$$

Replacing t by $1 - t$ in the righthand side of the above inequalities, we can readily obtain the corresponding improvements in the vicinity, $t \in [\frac{d-1}{d}, 1]$, of the other boundary point $\mathbf{r}(1) = \mathbf{b}_d$.

3 Optimal-orientation bounds

The various norms $\|\Delta_2 \mathbf{b}_i\|_p$, appearing in the bounds derived in the previous sections (see Thms. 2.1, 2.3 and 2.5) are, in general, orientation dependent. The question then naturally arises if it is possible to develop efficient techniques for determining, given a Bézier curve, the proper orientation of the coordinate system for which such a norm is minimal.

In the rest of this section we shall restrict ourselves to the bounds of Theorems 2.1 and 2.5, for their structure is analytically simpler in comparison to that of Theorem 2.3: the influence of the $\beta_{ki}(t)$'s is decoupled from that of the $\|\Delta_2 \mathbf{b}_i\|$'s. In addition, since $\|\Delta_2 \mathbf{b}\|_{\infty p} \leq \|\Delta_2 \mathbf{b}\|_{1p}$ (cf. (10), (11)), this section will develop techniques for minimizing $F_p(\theta) := \|\Delta_2 \mathbf{b}^\theta\|_{\infty p}$, and $G(\theta) := \|\Delta_2 b_x^\theta\|_\infty + \|\Delta_2 b_y^\theta\|_\infty$, where the superscript θ denotes the value of a quantity after the coordinate system has been rotated by an angle θ.

It is easy to verify that the functions $F_p(\theta)$ are periodic with period $\pi/2$, and that the function $G(\theta)$ is periodic with period π. We thus only need to look in the interval $[0, \pi/2]$ (resp. $[0, \pi]$) to find the minimum of $F_p(\theta)$ (resp. $G(\theta)$). In this connection, let $F_{p,min} := \min_{\theta \in [0,\pi/2]} F_p(\theta)$, $G_{min} := \min_{\theta \in [0,\pi]} G(\theta)$. The ensuing theorem guarantees that the smallest norm is obtained by minimizing $F_\infty(\theta)$. Using the, easily provable, relations $F_\infty(\theta) \leq F_p(\theta) \leq F_q(\theta), \theta \in [0, \pi/2]$ and $F_\infty(\theta) \leq G(\theta) \leq 2F_\infty(\theta), \theta \in [0, \pi]$, and taking the minimum over the angles θ, leads to

Theorem 3.1 *For any $p \geq q \geq 1$ we have $F_{\infty,min} \leq F_{p,min} \leq F_{q,min}$ and $F_{\infty,min} \leq G_{min} \leq 2F_{\infty,min}$.*

3.1 Minimizing $G(\theta)$

The aim is to determine the angles θ for which either (i) the argument of the maximum of either $\|\Delta_2 b_x^\theta\|_\infty$ or $\|\Delta_2 b_y^\theta\|_\infty$ changes, or (ii) $G(\theta)$ becomes zero. These values split the $[0, \pi]$ into intervals, with the property that, in each interval, $G(\theta)$ is of the form $|a \cos\theta + b \sin\theta|$ and convex downwards. Here a and b are linear functions of the coordinates of the vectors $\Delta_2 \mathbf{b}_i$. The minimum of $G(\theta)$ in each one of these intervals is the minimum of the values of $G(\theta)$ at the endpoints of the interval. We can then find the global minimum of $G(\theta)$ in $[0, \pi]$ by taking the minimum over those values.

The critical angular values, i.e., the values of θ for which the representation of $G(\theta)$ changes, are solutions of equations of the form $g_1(\theta) := |a \cos\theta + b \sin\theta| - |c \cos\theta + d \sin\theta| = 0$. Let's proceed with the analysis of an equation of type $g_1(\theta) = 0$. Let $\cot\phi_1 = \frac{b}{a}$ and $\cot\phi_2 = \frac{d}{c}$. Then $g_1(\theta) = 0$ can be written as $|a||\cos\theta + \cot\phi_1 \sin\theta| - |c||\cos\theta + \cot\phi_2 \sin\theta| = 0$, or, in a more compact form, $g_2(\theta) := a'|\sin\theta'| - c'|\sin(\theta' + \phi')| = 0$, where $a' := \frac{|a|}{|\sin\phi_1|}$, $c' := \frac{|c|}{|\sin\phi_2|}$, $\theta' = \theta + \phi_1$ and $\phi' = \phi_2 - \phi_1$. We shall assume that $\phi' \neq 0$, i.e., $\phi_1 \neq \phi_2$. We are interested in roots of $g_2(\theta) = 0$ in $[0, \pi]$. $g_2(\theta) = 0$ has two roots in $[0, \pi]$, one in $(0, \pi - \phi')$ and one in $(\pi - \phi', \pi)$.

We can thus use any root finder like the *bisection*, *secant* or *false position* method to compute the unique root in the two intervals. As far as the original equation is concerned, let $\alpha_1 = 0$, $\alpha_4 = \pi$ and $\beta_i = \pi - \phi_i$ if $\phi_i > 0$, whereas $\beta_i = -\phi_i$ if $\phi_i < 0$ for $i = 1, 2$. Finally let $\alpha_2 = \min\{\beta_1, \beta_2\}$ and $\alpha_3 = \max\{\beta_1, \beta_2\}$. Then the roots of equation $g_1(\theta) = 0$ in $[0, \pi]$ are in the intervals (α_i, α_{i+1}), $i = 1, 2, 3$. Note that since we have at most two roots for equation $g_1(\theta) = 0$, one of these intervals does not contain a root of the equation in question.

Based on the analysis above we can compute G_{min} using the following algorithm.

Algorithm FindMin-G
1. Compute $G(0)$. Set $\theta_c \leftarrow 0$, $\theta_{opt} \leftarrow 0$. Find the indices i_∞ and j_∞ for which $|\Delta_2 b^{\theta_c}_{i_\infty x}| = \|\Delta_2 b^{\theta_c}_x\|_\infty$, $\quad |\Delta_2 b^{\theta_c}_{j_\infty y}| = \|\Delta_2 b^{\theta_c}_y\|_\infty$. Set $G_{min} \leftarrow G(0)$.
2. Set $\theta_{old} \leftarrow \theta_c$.
3. Solve the equations $|\Delta_2 b^{\theta}_{i_\infty x}| = |\Delta_2 b^{\theta}_{ix}|$, $\quad |\Delta_2 b^{\theta}_{j_\infty y}| = |\Delta_2 b^{\theta}_{jy}|$, for all $i \neq i_\infty$ and $j \neq j_\infty$, and find the minimum angle θ_{min} that is a solution of one of these equations that is greater than θ_{old}. If such a θ_{min} does not exist set $\theta_{min} \leftarrow \pi$.
4. Set $\theta_c \leftarrow \theta_{min}$ and update the value(s) of i_∞ and/or j_∞.
5. Set $G_{min} \leftarrow \min\{G_{min}, G(\theta_c)\}$ and update θ_{opt}.
6. If θ_c is equal to π return $\{\theta_{opt}, G_{min}\}$. Otherwise goto to step 2.

End FindMin-G

We assume that finding the root of equation $g_1(\theta) = 0$ and the evaluation of sinusoidal functions take $O(1)$ time. Then steps 2, 4, 5 and 6 of the procedure above take $O(1)$ time. Step 1 takes $O(d)$ time, since we have to compute $G(0)$ and identify i_∞ and j_∞. In step 3 we have to solve $2(d-2)$ equations yielding $4(d-2)$ angular values, of which we have to find the minimum that is greater than θ_{old}; this takes $O(d)$.

In order to determine the total running time of the algorithm FindMin-G we need to determine how many times the loop is executed. To answer this question we can think of $\|\Delta_2 b^{\theta}_x\|_\infty$ and $\|\Delta_2 b^{\theta}_y\|_\infty$ as the upper envelope of a set of functions. These functions are of the form $A(\theta) = \alpha\,|\sin(\theta - \phi)|$, $\alpha > 0$, defined over $[0, \pi]$. Since $a\cos\theta + b\sin\theta = \frac{a}{\sin\phi}\sin(\theta - \phi)$, $\quad \cot\phi = -\frac{b}{a}$ functions of the form $A(\theta)$ defined over $[0, \pi]$, consist of at most two arcs of the form $\sin\theta$, $\theta \in [0, \pi]$, translated on the x-axis and scaled along the positive y-axis (actually we refer to the restriction of these arcs in $[0, \pi]$).

Let $A'(\theta; \alpha, \phi)$ denote the restriction in $[0, \pi]$ of an arc of the form $\sin\theta$, $\theta \in [0, \pi]$, translated on the x-axis by ϕ and scaled along the y-axis by α. Then $\|\Delta_2 b_x^\theta\|_\infty$ or $\|\Delta_2 b_y^\theta\|_\infty$ is the upper envelope of at most $2(d-1)$ arcs of the form $A'(\theta; \alpha, \phi)$. Let S_x be the set of these arcs for $\|\Delta_2 b_x^\theta\|_\infty$ and S_y be the set of these arcs for $\|\Delta_2 b_y^\theta\|_\infty$. Clearly, $|S_x| \le 2(d-1)$ and $|S_y| \le 2(d-1)$, and note that any pair of arcs in S_x or S_y have at most one intersection point.

The number of iterations in the algorithm described above is of the same order with the complexity of the sum of the upper envelopes of the sets S_x and S_y. The complexity of the upper envelope of a set S of x-monotone arcs, every pair of which have at most s intersection points is known to be $\lambda_{s+2}(|S|)$ (see [3, Corollary 1.6]), where $\lambda_s(n)$ is the length of an (n, s) *Davenport-Schinzel sequence* (see [3, Definition 1.1]). In our case $s = 1$. Hence the complexity of the upper envelopes of interest are $\lambda_3(|S_x|)$ and $\lambda_3(|S_y|)$. It is known that $\lambda_3(n) = O(n\alpha(n))$, where $\alpha(n)$ is the functional inverse of the Ackermann's function (see [3, Corollary 2.16]), which along with the fact that $|S_x|, |S_y| = O(d)$ implies that $\lambda_3(|S_x|), \lambda_3(|S_y|) = O(d\alpha(d))$. Since the complexity of the sum of two upper envelopes is the sum of the complexities of the upper envelopes, we conclude that the complexity of G, seen as an upper envelope, is $O(d\alpha(d))$. Hence the number of iterations that algorithm FindMin-G performs is $O(d\alpha(d))$, which gives a total running time of $O(d^2\alpha(d))$.

3.2 Minimizing $F_\infty(\theta)$

Let $\Delta_2 c_i^\theta = \Delta_2 b_{ix}^\theta$, $1 \le i \le d-1$, and let $\Delta_2 c_{i+d-1}^\theta = \Delta_2 b_{iy}^\theta$, $1 \le i \le d-1$. It is then easy to verify that $F_\infty(\theta) = \max_{1 \le i \le 2(d-1)} |\Delta_2 c_i^\theta|$. But $|\Delta_2 c_i^\theta|$ is of the form $|a\cos\theta + b\sin\theta|$, and we can use all the machinery developed so far for functions of this form. In particular, computing $F_{\infty,min}$ is essentially computing the minimum of the upper envelope of the functions $|\Delta_2 c_i^\theta|$. We can do that by the algorithm described below.

Algorithm FindMin-F_∞

1. Compute $F_\infty(0)$. Set $\theta_c \leftarrow 0$, $\theta_{opt} \leftarrow 0$. Find the index i_∞, for which $|\Delta_2 c_{i_\infty}^{\theta_c}| = \|\Delta_2 \mathbf{b}^{\theta_c}\|_{\infty\infty}$, where $\theta = \theta_c$. Set $F_{\infty,min} \leftarrow F_\infty(0)$.
2. Set $\theta_{old} \leftarrow \theta_c$.
3. Solve the equations $|\Delta_2 c_{i_\infty}^\theta| = |\Delta_2 c_i^\theta|$ for all $i \ne i_\infty$, and find the minimum θ_{min} that is a solution of one of these equations that is greater than θ_{old}. If such a θ_{min} does not exist set $\theta_{min} \leftarrow \pi/2$.
4. Set $\theta_c \leftarrow \theta_{min}$ and update the value of i_∞.

5. Set $F_\infty \leftarrow \min\{F_{\infty,min}, F_\infty(\theta_c)\}$ and update θ_{opt}.
6. If θ_c is equal to $\pi/2$ return $\{\theta_{opt}, F_{\infty,min}\}$. Otherwise, goto to step 2.

End FINDMIN-F_∞

As in algorithm FINDMIN-G, steps 2, 4, 5 and 6 take $O(1)$ time. Step 1 takes $O(d)$ since we need to compute $F_\infty(0)$ and determine i_∞. Step 3 takes $O(d)$ time as well, since we need to solve $2(d-1)-1$ equations and find the minimum of their roots that is greater than θ_{old}. The total running time depends on the number of iterations executed. This is equal to the complexity of the upper envelope of the functions $|\Delta_2 c_i^\theta|$. Each one of these functions consists of 2 arcs of the form $A'(\theta;\alpha,\phi)$. Let S be the set of these arcs. Then clearly $|S| \leq 4(d-1)$ and the complexity of the upper envelope of S is $\lambda_3(|S|) = O(d\alpha(d))$. Hence the total running time of FINDMIN-F_∞ is the same as that of FINDMIN-G, i.e., $O(d^2\alpha(d))$.

4 Polygonal envelopes

This section illustrates the use of the results and techniques presented in the previous sections, for constructing tight polygonal envelopes of planar polynomial curves. Given a Bézier curve $\mathbf{r}(t) = \sum_{i=0}^{d} \mathbf{b}_i B_i^d(t)$, $t \in [0,1]$, of degree d, such an envelope $\mathsf{E}(\mathbf{r}(t);p,c)$ can be represented as the Minkowski sum, denoted by $\bigoplus$, of a polygonal curve and a closed planar set, namely:

$$\mathsf{E}(\mathbf{r}(t);p,c) = \ell(t) \bigoplus \{\mathbf{q} \in \mathbb{R}^2 : \ \|\mathbf{q}\|_p \leq c\}, \tag{28}$$

where $\ell(t)$ is the parameterization (1) of the control polygon $\mathbb{L}$ of $\mathbf{r}(t)$ and c is the constant appearing in the right-hand side of the inequality we use for bounding the distance between the curve and its control polygon, measured by $\|\mathbf{r}(t) - \ell(t)\|_{\infty,p,[0,1]}$; see Thms. 2.1 and 2.5.

Fig. 1(a) depicts a 6-th degree ($d = 6$) Bézier curve (thick solid line) with its control polygon (thin solid line), enclosed by four different polygonal envelopes $\mathsf{E}(\mathbf{r}(t);p,c)$, constructed via (28). Analytically, the dotted and dashed envelopes are obtained by using the bound (9) of Theorem 2.1 with $r = \infty$ and $p = 1$ (dotted envelope) or $p = \infty$ (dashed envelope). The dash-dotted envelope results from the bound (23) of Theorem 2.3 with $p = \infty$. Finally, the solid envelope is constructed as the Minkowski sum $\mathsf{E}(\mathbf{r}(t); p = \infty, c_x, c_y) = \ell(t) \bigoplus \{\mathbf{q} = (q_x, q_y)^T \in \mathbb{R}^2 : \ |q_\bullet - \ell_\bullet| \leq c_\bullet, \bullet = x, y\}$, with c_x, c_y being the constants appearing in the univariate bounds in [1, Th. 3.1]

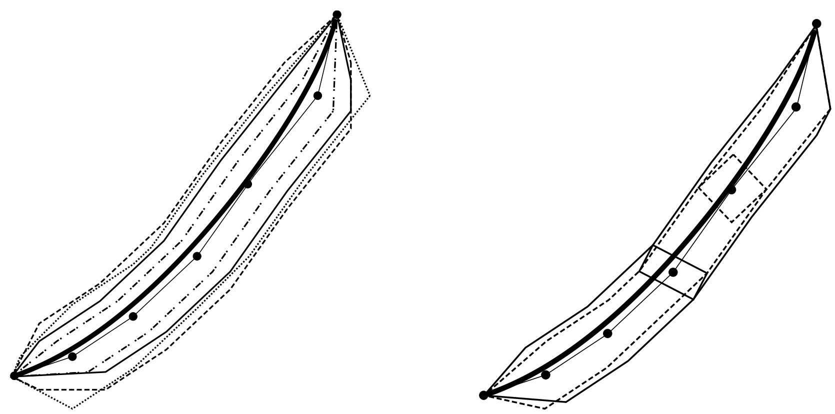

(a) (b)

Figure 1: (a)A Bézier curve (thick solid line) enclosed by four polygonal envelopes constructed with the aid of the bounds provided by Theorem 2.1 (dotted and dashed envelopes), Theorem 2.5 (dash-dot envelope) and [1, Th. 3.1] (solid envelope). (b) Optimizing the orientation angle for the dashed and solid envelopes in Fig. 1(a).

when applied to the x- and y-components of $\mathbf{r}(t)$, respectively. Note that all four envelopes have been improved at the ends with the aid of the endpoint-specific bounds at the end of §2, and, as far as the solid envelope is concerned, with the endpoint-specific bounds in [1, §8].

Minkowski sums were implemented using Alan Murta's *general polygon clipping*[2] library. For each line segment of the control polygon the Minkowski sum is a convex polygon with 4 or 6 sides. The Minkowski sum for the entire control polygon is computed as the union of the 4- or 6-sided convex polygons.

Fig. 1(b) depicts the dashed and the solid polygonal envelope of the curve in Fig. 1(a) after finding the orientation angles for which the corresponding norms $\|\Delta_2(b)\|_{\infty\infty}$ and $\|\Delta_2 b_x\|_\infty + \|\Delta_2 b_y\|_\infty$ become minimal. The minimization problems are solved by the algorithms FINDMIN-F_∞ and FINDMIN-G, respectively. Comparing the dashed and the solid envelopes in Figs. 1(a) and 1(b), it is readily seen that the *optimal-orientation* dashed envelope is definitely tighter than the corresponding one in Fig. 1(a).

Note that the polygonal envelopes one can construct via the bounds and optimization techniques presented in §2 and §3, can be rendered tighter if we take their intersection with the convex hull (CH) of the curve. This is

[2]GPC Homepage: `http://www.cs.man.ac.uk/aig/staff/alan/software/`

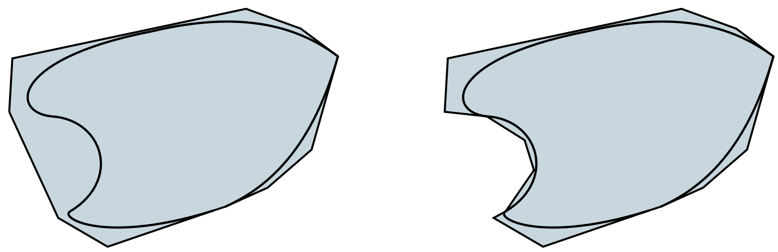

(a) (b)

Figure 2: (a) Convex hull bound. (b) Combining the convex hull with the polygonal envelope $\min_\theta \|\Delta_2 \mathbf{b}^\theta\|_{\infty\infty}$.

illustrated in Fig. 2, where we seek to construct an outer envelope for a closed composite curve (thick solid line), consisting of five simple Bézier pieces. The final envelope (see Fig. 2(b)) comprises a major part of the curve's CH (four out of the five pieces) and a part of the polygonal envelope, constructed via optimizing the norm $\|\Delta_2 \mathbf{b}^\theta\|_{\infty\infty}$. The CH bound is shown in Fig. 2(a).

References

[1] D. Nairn, J. Peters, and D. Lutterkort. Sharp, quantitative bounds on the distance between a polynomial piece and its bézier control polygon. *CAGD*, 16:613–631, 1999.

[2] U. Reif. Best bounds on the approximation polynomials and splines by their control structure. *CAGD*, 17:579–589, 2000.

[3] M. Sharir and P. K. Agarwal. *Davenport-Schinzel Sequences and Their Geometric Applications*. Cambridge University Press, New York, 1995.